Asian Journal of Chemistry; Vol. 35, No. 2 (2023), 493-498

ASIAN JOURNAL OF CHEMISTRY

https://doi.org/10.14233/ajchem.2023.26944

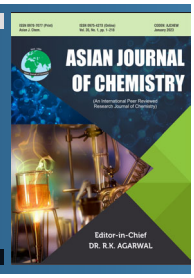

Fluorometric Detection of Al^{3+} Ion in Mixed Aqueous Solvent Based on Simple Schiff-Base Molecular Prob

SANJU DAS

Department of Chemistry, Maulana Azad College, Kolkata-700013, India

Corresponding author: E-mail: sanjudasju@gmail.com

Received: 22 November 2022; *Accepted*: 17 January 2023; *Published online*: 30 January 2023; AJC-21135

A simple fluorometric detection for Al^{3+} ion in mixed aqueous medium using a simple Schiff-base molecule through PET mechanism is discussed. The di-phenolic Schiff-base molecule (EAMHM) was synthesized by the condensation reaction of multiple phenolic aldehyde molecules with a diamine containing multiple aldehyde-reacting primary amine moieties. The extremely low fluorescence quantum yield for EAMHM is highly useful for the off-mode of fluorescence sensing purposes. Contrary to various other cations Ni^{2+}, Mg^{2+}, Co^{2+}, Cu^{2+}, Zn^{2+}, Cr^{3+}, Cd^{2+}, Fe^{3+}, Ba^{2+}, Hg^{2+}, the selective Al^{3+} ion induced large fluorescence enhancement can be employed to detect Al^{3+} even in the presence other bi- or tri-valent cations. Moreover, linear change in fluorescence intensity with Al^{3+} concentration is highly beneficial for ratiometric detection of unknown Al^{3+} concentrations. As revealed from various spectroscopic and theoretical calculations, EAMHM forms a 1:1 complex with Al^{3+} showing a large increase in fluorescence intensity. It has also been identified that efficient photo-induced electron transfer (PET) in free EAMHM is mainly responsible for its low fluorescence intensity, whereas the removal of such PET process during its complexation with Al^{3+} produces large fluorescence enhancement. The structural and electronic parameters of the free EAMHM and EAMHM-Al^{3+} complex have been analyzed using DFT-based theoretical calculations.

Keywords: Fluorometry, Aluminium ion, Mixed aqueous solvent, Photo-induced electron transfer, Schiff base.

INTRODUCTION

In the lithosphere, aluminium is one of the most available elements, which is widely used in the paper industry, electronic industry, pharmaceutical industry, food processing industry, *etc*. [1-3]. Beyond to the permissible limits, aluminum lead to disorders in people can lead to Alzheimer's, Parkinson's and dialysis encephalopathy, which are neurological diseases [4-6]. Humans are recommended to consume about 7 mg of Al^{3+} per kilogram of body weight per week, according to WHO recommendations [7]. In addition to retarding plant growth, it damages cellular membranes *via* oxidative damage. Although Al has several disadvantages, its mass usage in daily life can accumulate Al^{3+} and cause toxicity to humans and the environment. Aluminum increases the acidity of soil, so it is very fetal for the agricultural production [8]. On account of close relationship between aluminum and human health, there is an urgent need to develop a chemosensor for Al^{3+}.

Fluorescence method is more advantageous than other sophisticated methods as its operational simplicity, sensitivity, high selectivity, easy sample preparation and detection by both visual and instrumental methods and obviously for low cost [9,10]. Due to its weak coordinating abilities, Al^{3+} is more challenging to work with than other metals when it comes to making sensors [11]. As a result, Al^{3+} chemosensors in aqueous media require high selectivity and sensitivity.

Schiff bases are often used as chemosensors because they are easy to make and inexpensive [12-14]. For Al^{3+} chemosensors to work well in aqueous media, they need to be sensitive and selective. Thus, in this work, an attempt is made to construct a novel fluorescent 'turn-on' chemosensor for Al^{3+} ions based on simple Schiff-base molecule through PET mechanism. A diphenolic Schiff base molecule (EAMHM) was synthesized by the condensation reaction of multiple phenolic aldehyde molecules with a diamine containing multiple aldehyde reacting primary amine moieties.

EXPERIMENTAL

Commercially available reagents and solvents were procured from Sigma-Aldrich Chemicals Pvt. Ltd., USA, whereas

the spectroscopic grade solvent was purchased from E. Merck, India. The solvents were purified and dried by distillation procedure and used only after checking their purity fluorimetrically in the interest range of wavelength. Water (Milli-Q Millipore 18.2 MΩ cm^{-1}) was used throughout the study. Solvent mixture MeOH-HEPES buffer (25 mM, pH 7) (1:1 v/v) was used for all the spectroscopic measurements.

Characterization: LAMBDA 25 and LS-55 instruments (Perkin-Elmer, USA) were used for the UV-Vis absorption and fluorescence emission spectra, respectively. Quartz cells with a path length of 10 mm were used for absorption spectrum recording. For all measurements, the excitation wavelength was 365 nm, while the emission wavelength was between 8 and 3 nm. The fluorescence spectra were calibrated with respect to the instrumental response. To check the reproducibility, every spectroscopic measurement was conducted three times. An NMR spectrometer with a Bruker Advance DPX 300 MHz was used to measure ^{1}H NMR spectra in DMSO-d_6 with tetramethylsilane as an internal standard. Also, all the spectroscopic measurements were peformed with freshly made solutions, and the experiments were conducted at 25 ºC.

Synthesis of Schiff-base probe: 2-Hydroxy-3-(hydroxymethyl)-5-methylbenzaldehyde (HHMB) was synthesized from *p*-cresol with yield of 62% by following reported method [15]. To synthesize Schiff-base molecule 6,6′-(1Z,1′Z)-(ethane-1,2-diyl*bis*(azan-1-yl-1-ylidene))*bis*(methan-1-yl-1-ylidene)*bis*(2-(hydroxymethyl)-4-methylphenol) (EAMHM), ethylenediamine (EDA) (0.066 mL, 1 mmol) was added dropwise with constant stirring to a methanolic solution of HHMB (0.322 g, 2 mmol) followed by the addition 3 drops of acetic acid. The reaction mixture was then refluxed for 2.5 h at 45 ºC and finally the crude product was collected under reduced pressure. The product was purified by column chromatography to obtain deep yellow solid product and dried over $CaCl_2$ under vacuum (**Scheme-I**). ^{1}H NMR (DMSO-d_6, 300 MHz) δ ppm: 2.22 (s, 6H, Ar-CH_3), 2.49,3.31 (due to H_20 presence in DMSO-d_6), 3.83 (s, 4H, N-CH_2), 4.45 (s, 4H, CH_2-OH), 4.97 (s, 2H, CH_2-OH), 7.1-7.23 (s, 4H, Ar-H), 8.51 (s, 2H, imine-H), 13.41 (s, 2H, Ar-OH) ppm.

Determination of fluorescence quantum yield: The quantum yield of EAMHM as well as EAMHM-Al^{3+} were determined using standard method [16]. The standard fluorophore used was 9,10-diphenylanthracene in ethanol with emission quantum yield (ϕ_r) = 0.95. Using the following equation, the ϕ_f for the different systems was calculated:

$$\phi_{f_{sample}} = \frac{OD_{standard} \times A_{sample}}{OD_{sample} \times A_{standard}} \times \phi_{f_{standard}}$$

where, A_i is the absorbance at the excitation wavelength, F_i is the integrated emission area and n is the refractive index of solvent used. Subscripts refer to the reference (r) or sample(s) compound. The Schiff base EAMHM as well as EAMHM-Al^{3+} fluorescence spectra were recorded by 365 nm excitation at 25 ºC in 1:1 MeOH-HEPES buffer (v/v). At 450 nm fluorescence intensity band the quantum yield of EAMHM and EAMHM-Al^{3+} were determined 0.02 and 0.2, respectively.

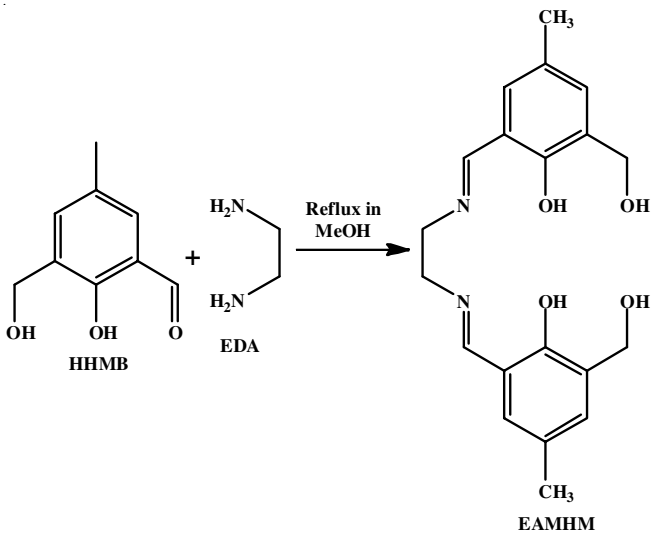

Scheme-I: Synthesis of the Schiff base molecule (EAMHM)

Theoretical calculation: By utilizing Gaussian 09, the ground state geometries of the probe (EAMHM) and its chelate complex with Al^{3+} were fully optimized in the gas phase to study their molecular and electronic structure [17]. The B3LYP functional with standard 6-31G basis set for all atoms had been adopted for this calculation. All of these species' global minima were confirmed using positive vibrational frequencies. The electrochemical properties of singlet excited states were investigated using B3LYP density functional theory (TD-DFT) based on the optimized geometry of their ground states (S_0). A ground state geometry was then evaluated with respect to excitation energies and respective oscillator strengths. Based on TD-DFT calculations, the UV-Vis spectra were calculated in a water medium between 250 and 650 nm. In aqueous medium, the conductor-polarized continuum model (CPCM) was adapted to calculate the fluorescence wavelength for the lowest singlet excited states using TD-DFT. Calculations based on theoretical models were found to reproduce experimentally obtained trends satisfactorily.

RESULTS AND DISCUSSION

UV-Vis studies: The UV-Vis absorption spectrum of the Schiff base ligand (EAMHM) was recorded at 25 ºC in 1:1 aqueous-methanol solution showing two well-defined intensity maxima at ~ 330 and 420 nm, respectively (Fig. 1a). It has been shown that the visible absorption intensity appears due to formation of deprotonated phenolate chromophore due to solvent polarity induced ground state proton transfer reaction from phenolic-OH to adjacent imine-N to generate partially charge separated zwitterionic species [18], while 330 nm intensity indicates that the second phenol-moiety remain as protonated form. The Schiff-base molecule containing multiple N- and O-centers (EAMHM) produces large affinity to interact various metal ions. To monitor the metal ion-induced complexation reaction for EAMHM, the changes in UV-Vis absorption for EAMHM were investigated in presence of various metal ions, such as Al^{3+}, Ni^{2+}, Mg^{2+}, Co^{2+}, Cu^{2+}, Zn^{2+}, Cr^{3+}, Cd^{2+}, Fe^{3+}, Ba^{2+}, Hg^{2+} (Fig. 1b). Interestingly, the absorption intensity profile

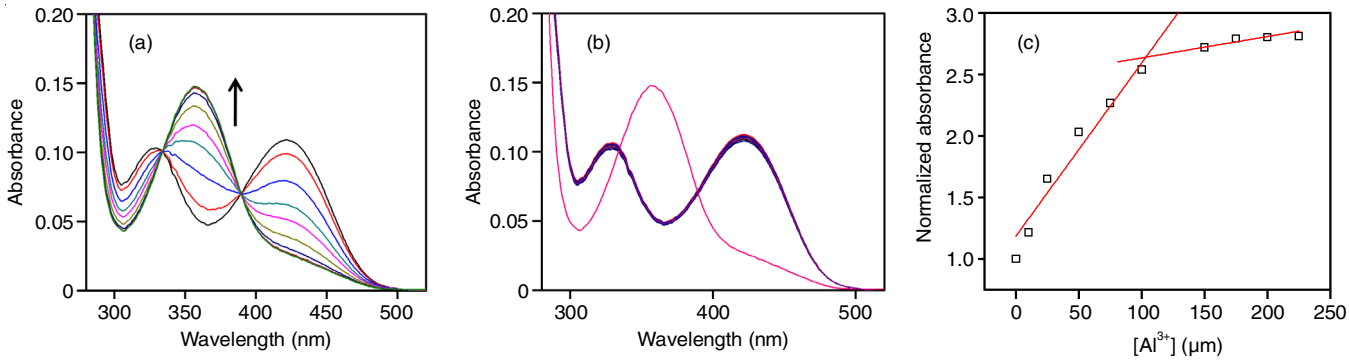

Fig. 1. (a) UV-Vis absorption spectra of EAMHM (25 mM) in 1:1 methanol-HEPES buffer solvent mixture with increasing concentration of Al^{3+} ion (0-225 μM); the changes in absorbance on addition of Al^{3+} is depicted by arrow. (b) The spectra in presence of various metal ions (10 equiv. w.r.t. Al^{3+}) are depicted. Black and pink spectra are for bare ligand EAMHM and in presence of Al^{3+} ion respectively. (c) Plot of normalized absorbance as a function of Al^{3+} ion concentration at 365 nm

of the EAMHM remains almost unchanged in presence of those various individual ions except Al^{3+}. It has been observed that both 330 and 420 nm absorption intensity for EAMHM gradually decreases with concomitant formation of new absorption intensity centered at ~ 365 nm until saturation was observed in presence of 9-equivalents of Al^{3+} ions (Fig. 1a). Most importantly, the appearances of two different isosbestic wavelengths ~ 334 and 390 nm justify a formation of new molecular species between Al^{3+} and EAMHM. Therefore, it has been considered that the Schiff-base molecule involved in complexation only with Al^{3+} ions among those various metal ions and the saturation in the absorption profile originated because of no other free EAMHM molecule present in solution to participate any further complexation reaction. The Al^{3+} ion-induced such change in UV-Vis absorbances of EAMHM may be useful for detection of Al^{3+} in aqueous solution. To observe the sensing applicability, the normalized 365 nm absorption intensities (normalized by 365 nm absorption intensity in absence of Al^{3+}) were plotted with the concentration of Al^{3+} ions and the linear correlation curve upto 4 equiv. of Al^{3+} is highly beneficial for detection of unknown Al^{3+} present in solution (Fig. 1c).

To identify the complex stoichiometry between EAMHM and Al^{3+}, absorbance related with the EAMHM-Al^{3+} complex was plotted against different mole fractions of Al^{3+}, while volume of solution had remained constant according to the Job's plot (Fig. 2) [19]. The maximum amount of complexation at 0.5 mole-fraction of Al^{3+} convincingly suggests the formation of 1:1 complex between EAMHM and Al^{3+} ions.

The influence of different anions to dissociate the EAMHM-Al^{3+} complex was also studied. A 365 nm absorption peak for the complex remains unperturbed in presence of various potential anions, such as Cl^-, BH_4^-, Br^-, NO_3^-, SCN^-, NO_2^-, CN^-, $S_2O_3^{2-}$ (Fig. 3b), which indicates that the complex is highly stable towards those anions. On the other hand, a notable change of absorption was identified in presence of 10 equiv. of S^{2-} (Fig. 3a). More specifically, an identical spectrum between the final absorption spectrum of the complex in presence of saturated S^{2-} ion and EAMHM clearly suggests that Al^{3+} is displaced as insoluble Al_2S_3 from the complex to generate free EAMHM.

Fluorometric detection: The fluorometric studies for EAMHM with or without the presence of various metal ions

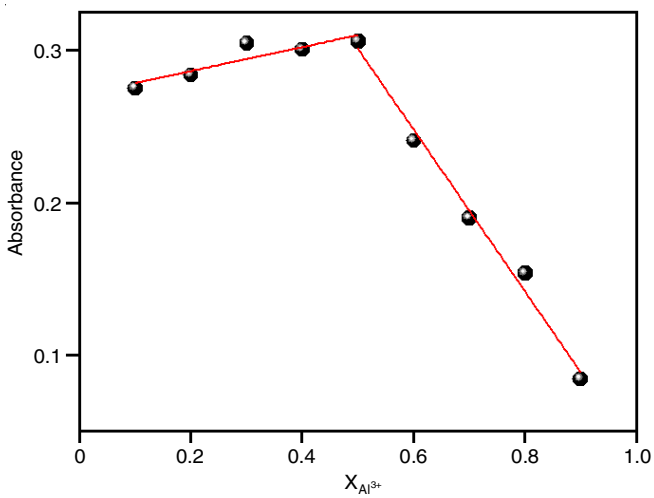

Fig. 2. Job's plot for determining the stoichiometry of the complex between EAMHM and Al^{3+} ion. The difference between the observed and EAMHM absorbance at 365 nm were plotted with mole fraction of Al^{3+} in the mixture of EAMHM and Al^{3+} with various compositions

were performed by maintaining conditions identical to that of absorption studies in 1:1 methanol/buffer mixed solvent medium. The Schiff-base molecule (EAMHM) shows very weak fluorescence intensity centered at ~ 510 nm (relative $\phi_F < 0.01$) for 420 nm excitation (Fig. 4a), whereas the molecule behaves completely non-fluorescent due to excitation by 330 nm light. The results indicates that the zwitterionic residue containing phenolate-conjugated with protonated imine is responsible for weak fluorescence intensity, however, the protonated phenol conjugated with imine moiety in the other half of molecule is completely non-fluorescent in nature. The extremely low fluorescence intensity of EAMHM is highly useful for its application as off-mode of fluorescence sensing. As a fluorescent sensor in aqueous media, EAMHM may be detected by enhancing its fluorescence with a suitable external reagent in its "on" mode.

As the concentration of Al^{3+} was increased in presence of 25 mL of Schiff base (EAMHM), a significant increase of fluorescence centered at 450 nm was observed. It reached saturation at 10 equiv. in 1:1 methanol/buffer (20 mM HEPES) medium (pH 7.0) (Fig. 4a). This indicates that the EAMHM-Al^{3+} complex may be responsible for the large fluorescence enhancement

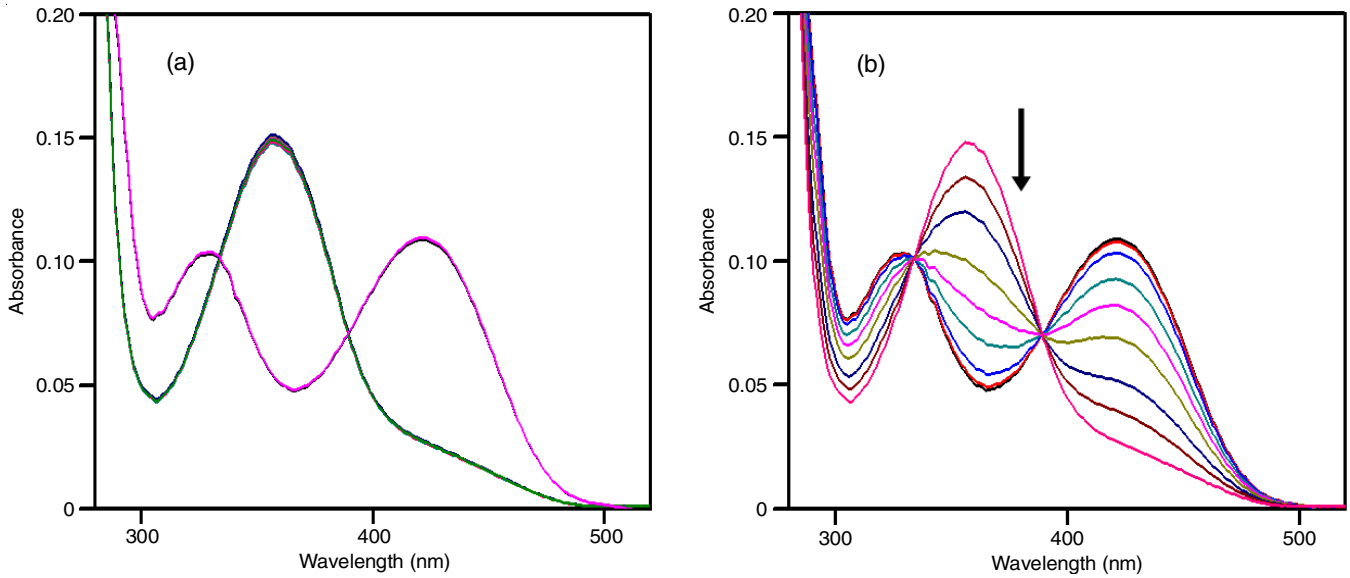

Fig. 3. UV-Vis absorption spectra of EAMHM-Al^{3+} in 1:1 methanol-HEPES buffer solvent mixture (a) with increasing concentration of S^{2-} ion (0-250 mM); the changes in absorbance on addition of S^{2-} is depicted by arrow. (b) In presence of different anions (10 equiv. w.r.t. S^{2-}). Black and magenta spectra are for bare ligand EAMHM and EAMHM-Al^{3+} in presence of S^{2-} respectively

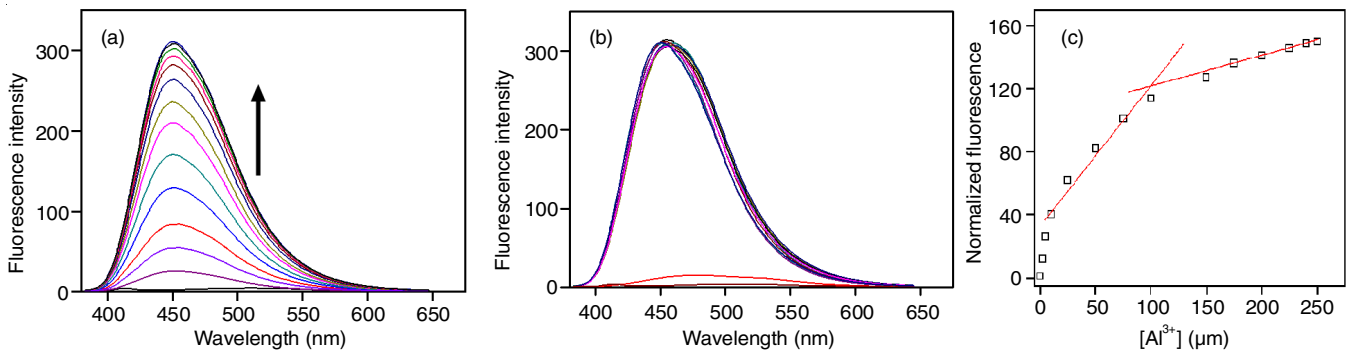

Fig. 4. Changes in the fluorescence spectra of EAMHM (25 μM) in 1:1 HEPES buffer-methanol solvent mixture (a) with increasing concentration of Al^{3+} ion (0-250 μM); the changes in fluorescence intensity on addition of Al^{3+} ion is depicted by arrow. (b) in presence of different anions (10 equiv. w.r.t. S^{2-}): wine, bare ligand EAMHM; red, EAMHM-Al^{3+} in presence of S^{2}. Excitation wavelength was 365 nm. (c) Plot of normalized fluorescence as a function of Al^{3+}ion concentration at 450 nm

since the amount of Al^{3+} required for fluorescence saturation is equal to that required for UV-Vis intensity saturation. When reaching saturation, Al^{3+} generated a 150-fold increase in the fluorescence at 365 nm (Fig. 4a).

Using DFT-based theoretical calculations, the low fluorescence intensity of free ligand (EAMHM) is due to the electron delocalization process (PET) caused by phenoxide oxygen atoms delocalizing electrons to a π-conjugated system of two aromatic rings and imino groups. There is a large increase in fluorescence intensity in the presence of Al^{3+} ions, which is likely due to the PET process being restricted efficiently to the EAMHM. Due to the reduction of electron-accepting abilities of the two aromatic rings and imine groups in the EAMHM-Al^{3+} coordinated complex, the PET process within the ligand would become weak. Additionally, the redshift of the emission wavelength of Schiff base ligand to 450 nm is also peculiar to the intensity of fluorescence emitted by Al^{3+} complexes [20]. A trace amount of Al^{3+} in an analytical medium can be detected by the large fluorescence intensity caused by Al^{3+}.

To verify Al^{3+} selectivity, the fluorescence of EAMHM (25 μM) was monitored individually in presence of different biologically or industrially important cations *viz*. Ni^{2+}, Mg^{2+}, Co^{2+}, Cu^{2+}, Zn^{2+}, Cr^{3+}, Cd^{2+}, Fe^{3+}, Ba^{2+}, Mg^{2+}, Hg^{2+} Na^{+}, Ca^{2+}, K^{+}, Fe^{2+} (~ 10 equivalent each w.r.t. Al^{3+}) in 1:1 methanol/buffer (20 mM HEPES) medium, pH 7.0 (Fig. 5) but failed to generate any noticeably enhanced fluorescence with an exception for the Al^{3+} ion with a very small fluorescence increment for the same cations. Interestingly, Al^{3+} induced fluorescence increment was not disturbed in presence of various other cations under identical solvent composition (Fig. 5). It is also important for Al^{3+} detection in the presence of other cations to have an unperturbed ratiometric response for EAMHM in the presence of large excess of those cations. In addition to limit of detection (LOD) of 1.0 M obtained, it is noteworthy that a trace amount of Al^{3+} can be detected with this LOD.

To determine the binding stoichiometry between Schiff base EAMHM and Al^{3+} as well as the binding constant, Benesi-Hildebrand procedure was adopted [21], where the change in

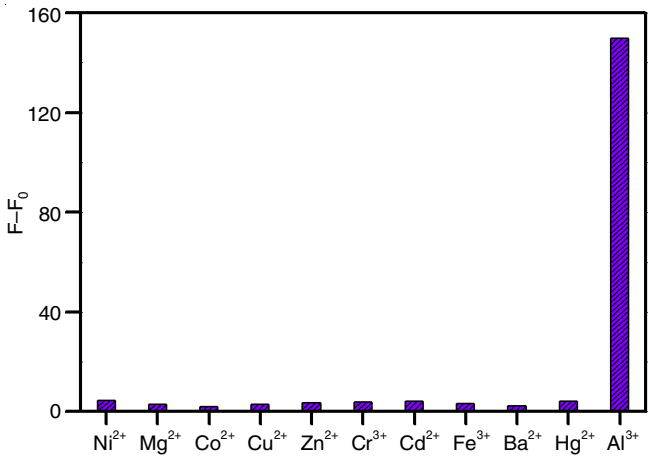

Fig. 5. Bar diagram indicating the Al^{3+} selective fluorescence increase over other metal ions

fluorescence intensity factor $((F_{max}-F_0)/(F_x-F_0))$ shows linear relation with inverse of Al^{3+} concentration indicating 1:1 binding stoichiometry between EAMHM and Al^{3+} (Fig. 6). On the other hand, the binding constant $(k_a) \sim 3.4 \times 10^4\ M^{-1}$ was determined from the slope value $\sim 2.99 \times 10^{-5}$ M.

$$\frac{(F_{max}-F_0)}{(F_x-F_0)} = 1 + \left(\frac{1}{K_a[C]^n}\right) \quad (1)$$

where, F_{max}, F_0 and F_x are fluorescence intensities of ligand in the presence of Al^{3+} at saturation, free ligand and any intermediate Al^{3+} concentration at $\lambda_{max} = 450$ nm. K_d is the dissociation constant of the EAMHM-Al^{3+}complex and concentration of Al^{3+} is represented by C. The binding constant (k_a) of the complex has been determined using the following relation:

$$k_a = \frac{1}{k_d}$$

As similar to the UV-Vis absorption studies, the quenching of fluorescence intensity due to dissociation of EAMHM-Al^{3+}

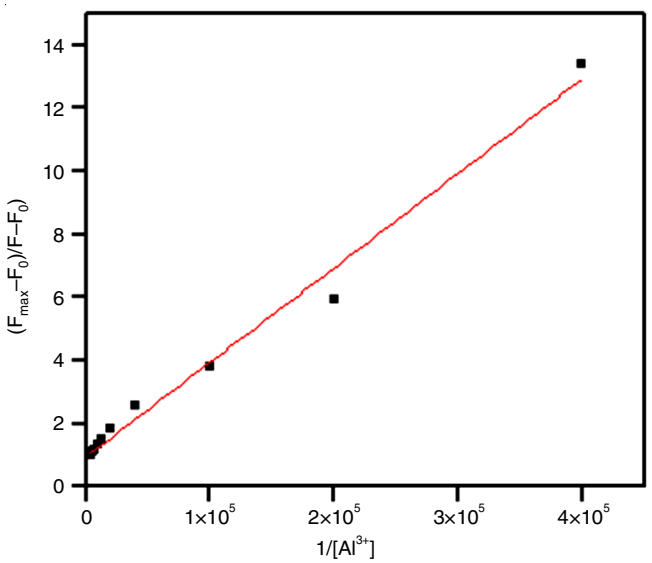

Fig. 6. Benesi-Hildebrand plot of $(F_{max}-F_0)/(F-F_0)$ *vs.* $1/[Al^{3+}]$ (obtained from emission spectra) shows a linear relationship with an intercept of about 0.95 ± 0.1 (close to 1.0) (λ_{ex} = 365 nm)

complex in presence of various anions, such as Cl^-, BH_4^-, Br^-, NO_3^-, SCN^-, NO_2^-, CN^-, $S_2O_3^{2-}$ and S^{2-} was monitored by the fluorescence method (Fig. 4b). Except in presence of S^{2-} anion, almost unchanged fluorescence intensity clearly justifies the complex is highly stable and it can be used as a fluorescence sensor for the detection of Al^{3+} in presence of those anions. Whereas, in case of S^{2-}, almost complete quenching of the fluorescence to a same extent as that of free EAMHM may also indicate that such fluorescence quenching is resulted by the generation of free EAMHM ligand.

Notably, the S^{2-} induced selective fluorescence quenching is useful for detection of S^{2-} ion by observing such fluorescence quenching. Moreover, as similar to the UV-Vis absorption studies, the linear correlation of fluorescence intensity increase *vs.* Al^{3+} concentration can be utilized for ratiometric detection of Al^{3+} (Fig. 4c).

Theoretical calculations: Based on evidences, molecular formula of EAMHM-Al^{3+} for 1:1 complex as revealed from Job's plot analysis, the ground state geometry for most probable structure was optimized by DFT method for investigating the absorption to the singlet excited states *via* TD-DFT calculations in solvent MeOH (Fig. 7). In addition, similar calculation was performed for free EAMHM to justify for present consideration for the proposed structural geometry of the EAMHM-Al^{3+} complex. The geometry of complexes possess a distorted tetrahedral arrangement around the central metal ions. The optimized geometry of complex is represented in Fig. 7.

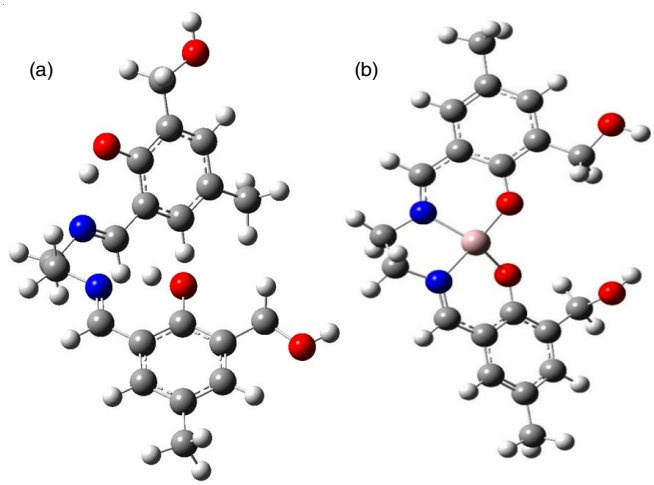

Fig. 7. Optimized ground state geometries of (A) EAMHM and (B) EAMHM-Al^{3+} complex

For EAMHM-Al^{3+} complex, a band around 362 nm is dominated by the HOMO–1(99) → LUMO (101) excitations, while the band around 377 nm for EAMHM is mainly due to HOMO (87) → LUMO (88) transitions. On comparing the experimental UV-Vis spectra for free EAMHM and EAMHM-Al^{3+} complex, it has been observed that the calculated electronic transitions are very close to the experimental electronic bands (Table-1).

Conclusion

In conclusion, a novel fluorescent 'turn-on' chemosensor EAMHM based on a Schiff base molecule containing multiple

TABLE-1
ELECTRONIC EXCITATION WAVELENGTH (nm), OSCILLATOR STRENGTHS (f_{cal}), ABSORPTION MAXIMUM (λ_{max}) AND EXTINCTION COEFFICIENT (ε) OF EAMHM AND EAMHM-Al^{3+} FORMS OBTAINED BY THE TD-DFT/B3LYP/6-31G++(d,p) CALCULATION ON GROUND STATE GEOMETRIES IN VARIOUS SOLVENT WITH CPCM DIELECTRIC SOLVATION MODEL. THE EXPERIMENTALLY OBTAINED UV-VIS ABSORPTION (Obs/Abs) PARAMETERS ARE DEPICTED FOR COMPARISON

	Form	Solvent	λ_{max} (nm)	f_{cal}	$\varepsilon \times 10^{-4}$ (M^{-1} cm^{-1})
TD-DFT	EAMHM	MeOH	377, 303	0.04, 0.21	0.42, 0.39
	EAMHM-Al^{3+}	MeOH	362	0.07	0.55
Obs/Abs	EAMHM	1:1 aqueous methanol	420, 330		0.44, 0.41
	EAMHM-Al^{3+}	1:1 aqueous methanol	365		0.59

phenol-conjugated-imine moieties derived from phenolic aldehyde and diamine molecule is developed . The EAMHM exhibits a high selectivity and sensitivity for the detection of Al^{3+} through significant visible fluorescence enhancement in the wavelength centered at 450 nm with a micromolar detection limit in CH_3OH/HEPES buffer (pH 7.0) binary solution mixture. The unperturbed Al^{3+} induced fluorescence enhancement by addition of different other cations justify that EAMHM molecule can be utilized for the detection of Al^{3+} in the presence of other competing metal ions also.

CONFLICT OF INTEREST

The authors declare that there is no conflict of interests regarding the publication of this article.

REFERENCES

1. S. Goswami, S. Paul and A. Manna, *RSC Adv.*, **3**, 10639 (2013); https://doi.org/10.1039/c3ra40984h
2. R.E. Doherty, *Environ. Forensics*, **1**, 83 (2000); https://doi.org/10.1006/enfo.2000.0011
3. M.S. Golub, J.M. Donald, M.E. Gershwin and C.L. Keen, *Neurotoxicol. Teratol.*, **11**, 231 (1989); https://doi.org/10.1016/0892-0362(89)90064-0
4. N. Fimreite, O.O. Hansen and H.C. Pettersen, *Bull. Environ. Contam. Toxicol.*, **58**, 1 (1997); https://doi.org/10.1007/s001289900292
5. H. Wang, B. Wang, Z. Shi, X. Tang, W. Dou, Q. Han, Y. Zhang and W. Liu, *Biosens. Bioelectron.*, **65**, 91 (2015); https://doi.org/10.1016/j.bios.2014.10.018
6. M. Iniya, D. Jeyanthi, K. Krishnaveni and D. Chellappa, *J. Lumin.*, **157**, 383 (2015); https://doi.org/10.1016/j.jlumin.2014.09.018
7. A. Budimir, *Acta Pharm.*, **61**, 1 (2011); https://doi.org/10.2478/v10007-011-0006-6
8. N.E.W. Alstad, B.M. Kjelsberg, L.A. Vollestad, E. Lydersen and A.B.S. Poleo, *Environ. Pollut.*, **133**, 333 (2005); https://doi.org/10.1016/j.envpol.2004.05.030
9. S. Kim, J.Y. Noh, K.Y. Kim, J.H. Kim, H.K. Kang, S.W. Nam, S.H. Kim, S. Park, C. Kim and J. Kim, *Inorg. Chem.*, **51**, 3597 (2012); https://doi.org/10.1021/ic2024583
10. Y. Lu, S. Huang, Y. Liu, S. He, L. Zhao and X. Zeng, *Org. Lett.*, **13**, 5274 (2011); https://doi.org/10.1021/ol202054v
11. M. Venturini-Soriano and G. Berthon, *J. Inorg. Biochem.*, **85**, 143 (2001); https://doi.org/10.1016/S0162-0134(01)00206-9
12. C. Pan, K. Wang, S. Ji, H. Wang, Z. Li, H. He and Y. Huo, *RSC Adv.*, **7**, 36007 (2017); https://doi.org/10.1039/C7RA05064J
13. S. Muthusamy, K. Rajalakshmi, D. Zhu, W. Zhu, S. Wang, K.-B. Lee H. Xue and L. Zhao, *Sens. Actuators B: Chem.*, **346**, 130534 (2021); https://doi.org/10.1016/j.snb.2021.130534
14. J. Ma, Y. Dong, Z. Yu, Y. Wu and Z. Zhao, *New J. Chem.*, **46**, 3348 (2022); https://doi.org/10.1039/D1NJ05919J
15. E. Lambert, B. Chabut, S. Chardon-Noblat, A. Deronzier, G. Chottard, A. Bousseksou, J.-P. Tuchagues, J. Laugier, M. Bardet and J.-M. Latour, *J. Am. Chem. Soc.*, **119**, 9424 (1997); https://doi.org/10.1021/ja970345q
16. J.V. Morris, M.A. Mahaney and J.R. Huber, *J. Phys. Chem.*, **80**, 969 (1976); https://doi.org/10.1021/j100550a010
17. M.J. Frisch, G.W. Trucks, H.B. Schlegel, G.E. Scuseria, M.A. Robb, J.R. Cheeseman, G. Scalmani, V. Barone, B. Mennucci, G.A. Petersson, H. Nakatsuji, M. Caricato, X. Li, H.P. Hratchian, A.F. Izmaylov, J. Bloino, G. Zheng, J.L. Sonnenberg, M. Hada, M. Ehara, K. Toyota, R. Fukuda, J. Hasegawa, M. Ishida, T. Nakajima, Y. Honda, O. Kitao, H. Nakai, T. Vreven, J.A. Montgomery, Jr., J.E. Peralta, F. Ogliaro, M. Bearpark, J.J. Heyd, E. Brothers, K.N. Kudin, V.N. Staroverov, R. Kobayashi, J. Normand, K. Raghavachari, A. Rendell, J.C. Burant, S.S. Iyengar, J. Tomasi, M. Cossi, N. Rega, J.M. Millam, M. Klene, J.E. Knox, J.B. Cross, V. Bakken, C. Adamo, J. Jaramillo, R. Gomperts, R.E. Stratmann, O. Yazyev, A.J. Austin, C. Pomelli, J.W. Ochterski, R.L. Martin, K. Morokuma, R. Cammi, V.G. Zakrzewski, G.A. Voth, P. Salvador, J.J. Dannenberg, S. Dapprich, A.D. Daniels, Ö. Farkas, J.B. Foresman, J. Cioslowski, J.V. Ortiz and D.J. Fox, Gaussian, Inc., Wallingford CT, , Gaussian 09 Rev. A.1 (2009).
18. Y. Sarkar, S. Das, A. Ray, S.K. Jewrajka, S. Hirota and P.P. Parui, *Analyst*, **141**, 2030 (2016); https://doi.org/10.1039/C5AN02128F
19. S. Biswas, S. Mukherjee, J. Bandyopadhyay, S. Samanta, I. Bhowmick, S. Das, D.K. Hazra, A. Ray and P.P. Parui, *RSC Adv.*, **4**, 9656 (2014); https://doi.org/10.1039/C4RA00069B
20. D. Maity and T. Govindaraju, *Eur. J. Inorg. Chem.*, **2011**, 5479 (2011); https://doi.org/10.1002/ejic.201100772
21. H.A. Benesi and J.H. Hildebrand, *J. Am. Chem. Soc.*, **71**, 2703 (1949); https://doi.org/10.1021/ja01176a030